FILE COPY
NO

CONFIDENTIAL

Copy No. 186

RM No. A8D27

CLASSIFICATION CANCELLED

NACA

RESEARCH MEMORANDUM

WIND-TUNNEL INVESTIGATION OF TRANSONIC AILERON FLUTTER OF A SEMISPAN WING MODEL WITH AN NACA 23013 SECTION

By Angelo Perone and Albert L. Erickson

Ames Aeronautical Laboratory
Moffett Field, Calif.

THIS DOCUMENT ON LOAN FROM THE FILES OF

NATIONAL ADVISORY COMMITTEE FOR AERONAUTICS
LANGLEY AERONAUTICAL LABORATORY
LANGLEY FIELD, HAMPTON, VIRGINIA

CLASSIFICATION CANCELLED
AUTHORITY H.L. DRYDEN CHANGE #1471
DATE 6-11-53 T.C. FRASER, JR.

RETURN TO THE ABOVE ADDRESS.

REQUESTS FOR PUBLICATIONS SHOULD BE ADDRESSED AS FOLLOWS:

NATIONAL ADVISORY COMMITTEE FOR AERONAUTICS
1512 H STREET, N. W.
WASHINGTON 25, D. C.

CLASSIFIED DOCUMENT

This document contains classified information affecting the National Defense of the United States within the meaning of the Espionage Act, USC 50:31 and 32. Its transmission or the revelation of its contents in any manner to an unauthorized person is prohibited by law. Information so classified may be imparted only to persons in the military and naval services of the United States, appropriate civilian officers and employees of the Federal Government who have a legitimate interest therein, and to United States citizens of known loyalty and discretion who of necessity must be informed thereof.

NATIONAL ADVISORY COMMITTEE FOR AERONAUTICS

WASHINGTON

July 12, 1948

CLASSIFICATION CANCELLED

CONFIDENTIAL

CLASSIFICATION CANCELLED

NATIONAL ADVISORY COMMITTEE FOR AERONAUTICS

RESEARCH MEMORANDUM

WIND-TUNNEL INVESTIGATION OF TRANSONIC AILERON FLUTTER OF A SEMISPAN WING MODEL WITH AN NACA 23013 SECTION

By Angelo Perone and Albert L. Erickson

SUMMARY

Presented herein are the results of a wind-tunnel investigation of aileron flutter up to 0.822 Mach number. The purpose of the tests was to investigate one-degree-of-freedom flutter of an aileron on a wing having an NACA 23013 section. The tests indicated the absence of flutter of significant amplitude when a considerable amount of wing-tip relief existed and the presence of flutter when the relief was minimized. The desirability of having as much of the aileron as possible in the relatively low-speed flow resulting from tip relief is discussed. The agreement that existed between the predicted and actual flutter frequency was sufficient to indicate that sections of the type tested will not alter the existing recommendations for flutter analysis. A normal variation of static aileron hinge-moment coefficient with aileron angle was found to exist at all the test Mach numbers.

INTRODUCTION

Most research on aileron flutter at transonic speeds conducted in the past has been with wings having low-drag sections. Considerable discussion has arisen concerning the possible effect of chordwise pressure-recovery gradient as a factor in control-surface flutter at high speeds. Since the NACA 23013 section has a relatively small pressure-recovery gradient compared to that of a low-drag section, its aileron flutter characteristics were investigated. A second aim of the tests was to compare the aileron flutter frequencies found experimentally with those predicted according to the theory developed in previous research. A third purpose of the tests involved studying the effects of minimizing wing-tip relief by use of an end plate to observe the effect on the flutter

characteristics. The model tested had an 8-foot semispan, an NACA 23013 airfoil section, and a round-nose aileron of 4-foot span with no aerodynamic balance. The tests were conducted in the Ames 16-foot high-speed wind tunnel.

COEFFICIENTS AND SYMBOLS

The symbols used in the analysis are defined as follows:

C_{h_a} aileron hinge-moment coefficient $\left(\frac{H}{q\, b_a\, \overline{c_a^2}}\right)$

H aileron hinge moment, foot-pounds

I aileron mass moment of inertia about the hinge line, inch-pound seconds squared

M Mach number $\left(\frac{V}{a}\right)$

M_{cr} critical Mach number of the NACA 23013 section

V airspeed, feet per second

a speed of sound, feet per second

b_a aileron span, feet

$\overline{c_a^2}$ mean square of aileron chord aft of hinge line, square feet

d distance from minimum pressure point on wing chord (coincident with average aileron chord) to trailing edge, feet

f aileron flutter frequency, cycles per second

f_a aerodynamic frequency $\left[\frac{a(1-M_{cr})}{4d}\right]$ cycles per second

q free-stream dynamic pressure $\left(\frac{1}{2}\rho V^2\right)$, pounds per square foot

α angle of attack of wing relative to air stream, degrees

δ_a aileron deflection, degrees

φ' phase angle between aileron displacement and resultant hinge moment, degrees
(Positive values indicate a leading hinge moment.)

ω flutter circular frequency, radians per second

MODEL AND APPARATUS

The model wing consisted of a steel box spar which was covered with mahogany plywood shaped to the NACA 23013 airfoil section. The aileron was constructed of wood ribs covered with mahogany veneer. Mass balance of the aileron was accomplished by means of lead weights forward of the hinge line. The aileron was of the round-nose, unsealed type with a 1/16-inch gap and had no aerodynamic balance. Pertinent dimensions of the model are included in the appendix.

The model mounted in the wind tunnel is shown in figure 1. A 5-percent-thick strut was used to support the wing tip during the tests to prevent, as nearly as possible, flutter of more than one degree of freedom. Figure 2 shows the end plate used to minimize spanwise flow near the wing tips, and the pertinent dimensions are shown in figure 3.

Control of the aileron was accomplished by means of a control-cable system, a schematic sketch of which is shown in figure 4. An electrical strain gage was fixed to the system to measure aileron hinge moment.

The aileron angle was measured by use of a slide-wire position indicator. A recording oscillograph was used to record fluctuations of aileron angle and aileron hinge moment.

METHOD

During the initial stage of testing, a study of the chordwise flow over the wing was conducted up to 0.822 Mach number by means of the shadowgraph method as outlined in reference 2. Tuft studies of the upper surface were also made. The remainder of the test was conducted with an end plate mounted at the wing tip for the purpose of minimizing the tip inflow observed during the tuft studies.

Time records of aileron deflection and aileron hinge moment were obtained on film by means of a recording oscillograph and the instantaneous values were read directly from these records. Parts of some of the records obtained are shown in figure 5.

The inertia of the aileron in still air with and without the mass balance weights was found by clamping the trailing edge to a spring system of known spring constant and finding the natural frequency of the system including the aileron. The inertia was then calculated according to the relation

$$I = \frac{K L^2}{4 \pi^2 f^2}$$

where K = constant of the spring system, L = distance from aileron hinge line to support of spring, f = frequency of oscillation of aileron.

The test Mach numbers were corrected for the constriction of the model and the tip support strut according to the method of reference 1.

RESULTS AND DISCUSSION

The results obtained and the accompanying discussion have been grouped in three sections: The first relates to the testing without an end plate, the second concerns the effects of an end plate, and the third is a comparison with empirical theory.

Without End Plate

In testing without an end plate, due to a faulty aileron position indicator, no usable oscillograph records of aileron deflection were obtained. In this phase of the testing there was no visually perceptible aileron flutter. The possibility that flutter of low amplitude may have occurred and gone unnoticed must not be overlooked. Compressibility effects as indicated by shadowgraphs were first noted at 0.685 Mach number with the formation of a small shock wave on the upper surface of the wing at about the 20-percent-chord location. With increase in Mach number, the wave moved aft on the wing and increased in strength. At 0.822 Mach number a strong shock wave was noticed at about the 50-percent-chord point on both the upper and the lower surfaces. These two waves oscillated fore and aft on the wing between approximately the 40- and 60-percent-chord points, indicating that fluctuating forces were present.

The results of the tuft studies are shown in figure 6(a) by use of arrows pointing in the direction of the air flow. The predominant feature in the flow was the inflow from the wing tip. The presence of this tip relief is important in that it produced relatively low-speed flow over about one-half of the aileron and served to lessen or prevent the extension of a shock wave from the inboard part of the wing all the way to the tip. So, even though flutter of this conventional section did not occur in the range of the tunnel tests, it cannot be construed, in light of the above evidence, that the type of wing section alone prevented flutter. The extent to which tip relief is effective depends on the amount of the aileron experiencing the effect of the low-speed flow. This criterion must be considered in any comparison of the flutter characteristics of the NACA 23013 section with those of the low-drag section reported in reference 2. Comparison of both semispan wings shows that, while the aspect ratios were equivalent, the conventional section had an aileron that extended over only one-half the model span; whereas the aileron of the low-drag section (reference 2) extended over almost the complete span tested, therefore subjecting a greater part of the control to strong compressibility effects. The advantage of a low aileron-span-to-wing-span ratio combined with low aspect ratio is thus evident in this case.

With End Plate

The purpose of utilizing the end plate was to subject as much of the aileron as possible to compressibility effects by extension of sonic velocities toward the wing tip. It should be noted that a similar effect could have been obtained by inward extension of the aileron. With the end plate, tuft studies (fig. 6(b)) indicated flow approaching a two-dimensional type over the wing and the subsequent extension of compressibility effects over the aileron. Under these conditions aileron flutter occurred at transonic airspeeds.

Oscillograph records of the aileron position indicated flutter at frequencies of between 16 and 20 cycles per second with amplitudes of not over 3.1°. (Amplitude as used throughout this report refers to total aileron motion.) In previous tests of a model with a low-drag section, motions as large as 20° resulted. It is difficult to account for the relatively small amplitudes of aileron flutter encountered in these tests of a conventional airfoil in a simple manner on the basis of this initial investigation. As a postulation, it is possible that the more favorable pressure gradient aft of the shock wave for the NACA 23013 section, relative to that of a low-drag section, may

be a contributing factor in producing flutter of a decidedly reduced amplitude. It is also possible that in this test, even with the end plate in place, the tip interference was sufficient to damp the aileron motion due to the relatively short aileron span. The flutter was, however, of a sufficiently violent nature to damage the aileron and terminate the tests. The flutter frequencies and the corresponding amplitudes for the different aileron moments of inertia and restraint conditions are listed in table I.

Figure 7 presents the variation of static aileron hinge-moment coefficient C_{h_a} with aileron angle δ_a at various Mach numbers. The dispersion of the experimental data at Mach numbers of 0.793 and 0.822 is due to fluctuations of the aileron position and hinge moment. Figure 8 presents the change of static aileron hinge-moment coefficient with change in aileron angle $\partial C_{h_a}/\partial\delta_a$ as a function of Mach number. A normal variation of $\partial C_{h_a}/\partial\delta_a$ existed at all Mach numbers with a less stable condition ($\partial C_{h_a}/\partial\delta_a$ less negative) from 0.75 to 0.822 Mach number.

Comparison With Theory

Comparison of the observed aileron flutter frequencies with the theory of reference 2 indicates good agreement. The flutter frequency was predicted using the relationship of equality of inertia force to aerodynamic force component for steady-state conditions.

That is,

$$I\omega^2 = \frac{\partial H}{\partial \delta_a} \cos \varphi'$$

where

$$\varphi' = \left(1 - \frac{f}{f_a}\right) 360^\circ$$

and

$$f_a = \frac{a(1-M_{cr})}{4d}$$

combining

$$I\omega^2 = \frac{\partial H}{\partial \delta_a} \cos \left\{ \left[1 - \frac{4\,fd}{a(1-M_{cr})}\right] 360^\circ \right\}$$

For the sake of simplicity the solution of the preceding equation for aileron flutter frequency was accomplished graphically. As both sides of the last equation are functions of the flutter frequency, this value was obtained by assuming a frequency for the inertia-force term $I\omega^2$ and solving for the frequency f in the aerodynamic-force component side of the equation. A plot of the initially assumed frequencies against those obtained by solution of the equation enabled the finding of the theoretical flutter frequency. The plot is included in figure 9. From this plot flutter frequencies of 20.6 and 21.4 cycles per second were predicted for the aileron with and without the balance weights, respectively. The experimental values of between 16 and 20 cycles per second are considered to be in reasonable agreement with the theory.

CONCLUSIONS

Tests of the semispan wing-aileron model with NACA 23013 sections indicated that:

1. The use of a control surface having a large portion of its span in a region of relatively low-speed flow arising from wing-tip relief may allevaite transonic flutter.

2. The conventional type of wing section, compared to low-drag sections, reduces the amplitude of the aileron flutter but does not prevent it.

3. The agreement that existed between the predicted and the actual flutter frequency was sufficient to indicate that sections of the type tested will not alter the existing recommendations for flutter analysis.

Ames Aeronautical Laboratory,
National Advisory Committee for Aeronautics,
Moffett Field, Calif.

APPENDIX

Dimensional Data

Wing

Span, feet	8.0
Area, square feet	31.0
Root chord, feet	5.05
Tip chord, feet	2.75
Airfoil section	NACA 23013
Aspect ratio	4.13

Aileron

Span, feet	4
Root chord, feet	0.980
Tip chord, feet	0.688
Area, square feet	3.34
Aileron inertia (no balance weights) pound–inch seconds squared	0.413
Aileron inertia (with balance weights) pound–inch seconds squared	0.719

REFERENCES

1. Herriot, John G.: Blockage Corrections for Three–Dimensional–Flow Closed–Throat Wind Tunnels, with Consideration of the Effect of Compressibility. NACA RM No. A7B28, 1947.

2. Erickson, Albert L., and Stephenson, Jack D.: A Suggested Method of Analyzing for Transonic Flutter of Control Surfaces Based on Available Experimental Evidence. NACA RM No. A7F30, 1947.

Table I.- Transonic flutter of an aileron on a semispan wing with an NACA 23013 section and equipped with an end plate.

Mach number, M	Aileron flutter frequency (cycles/sec)	Amplitude (deg)	Aileron moment of inertia (in-lb sec^2)	Remarks		
0.775	20.0	3.1	0.413	$\alpha = 2°$	aileron free	no static balance
0.775	17.0	1.6	0.413	$\alpha = 0°$	aileron free	no static balance
0.80	16.2	2.1	0.413	$\alpha = 0°$	aileron free	no static balance
0.775	16.4	2.3	0.719	$\alpha = 2°$	aileron free	statically balanced
0.775	18.6	2.1	0.719	$\alpha = 2°$	aileron free	statically balanced
0.775	17.0	2.4	0.719	$\alpha = 2°$	aileron free	statically balanced
0.775	18.9	1.8	0.719	$\alpha = 2°$	control cables loose	statically balanced

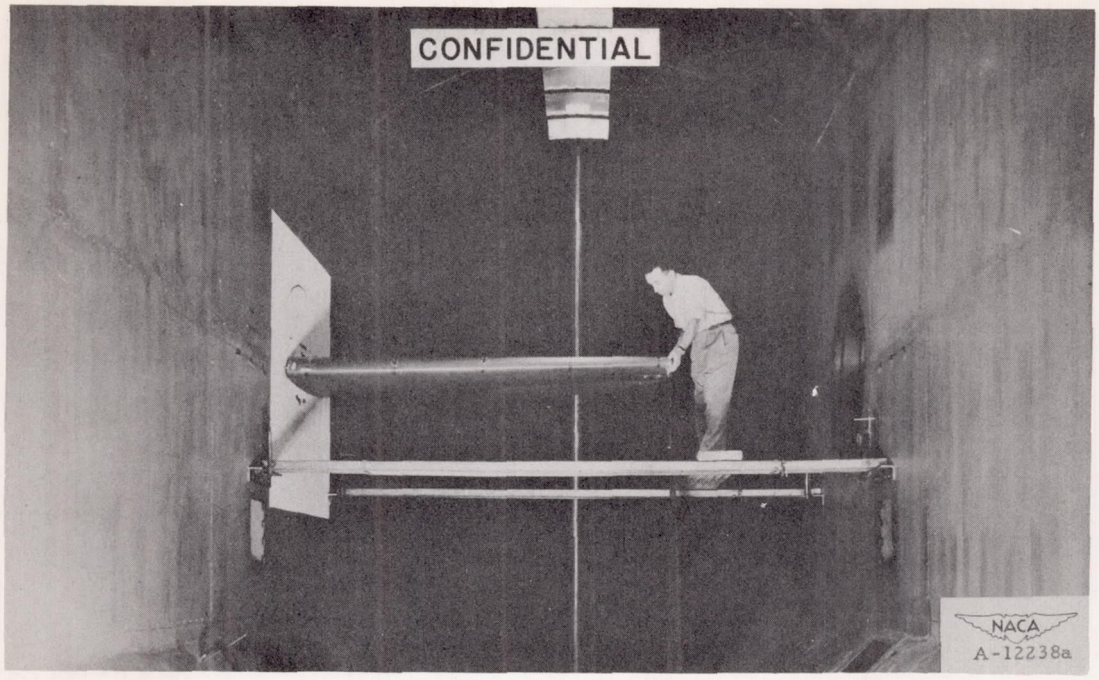

(a) Front view.

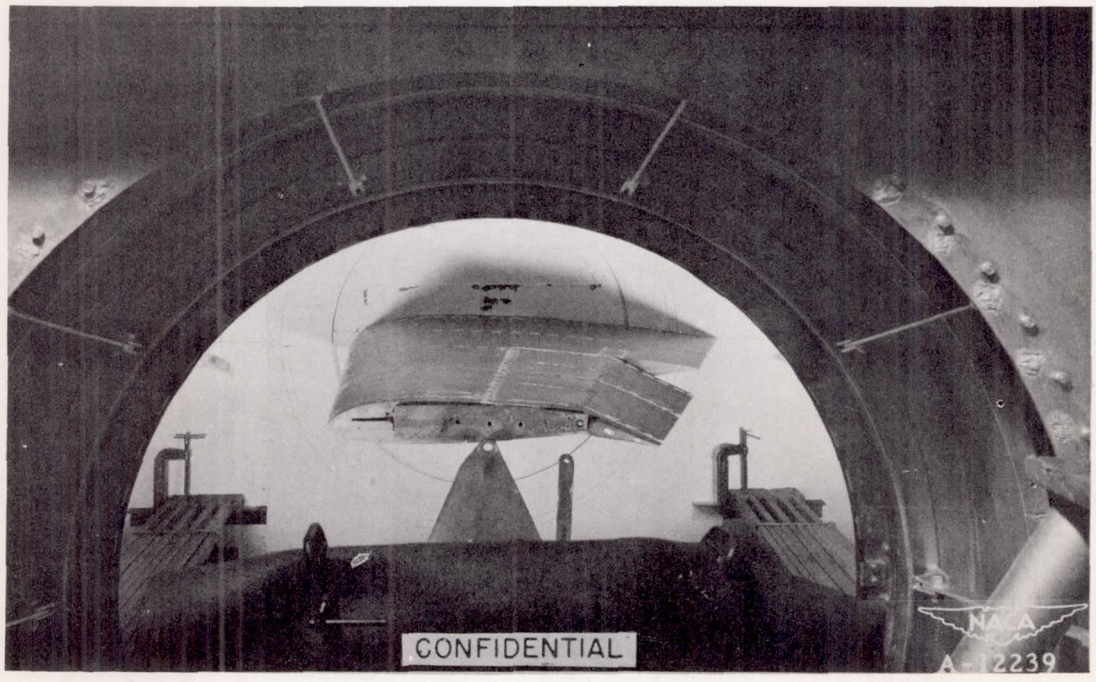

(b) End view.

Figure 1.- The NACA 23013 wing in the Ames 16-foot high-speed wind tunnel.

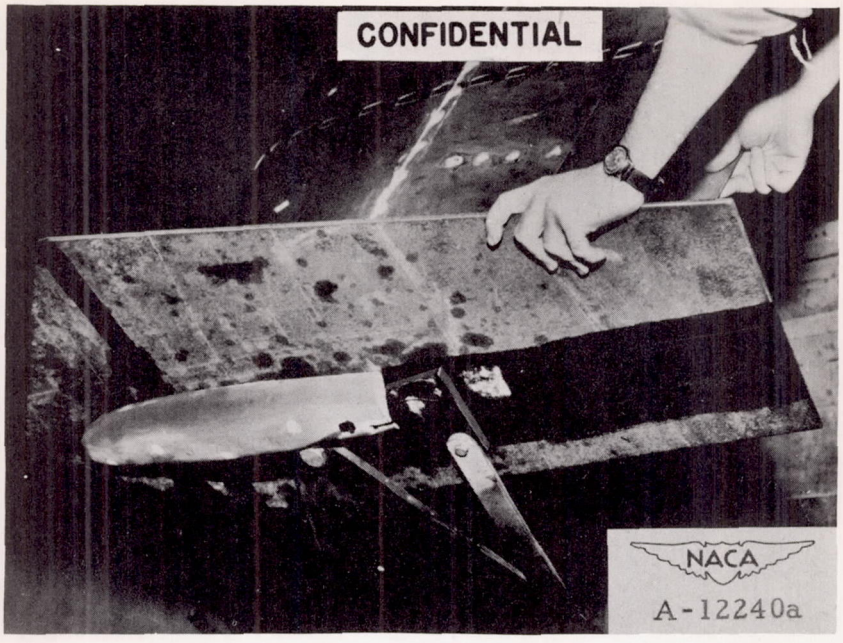

(a) End view.

(b) View looking outboard.

Figure 2.- The end plate in place on the model.

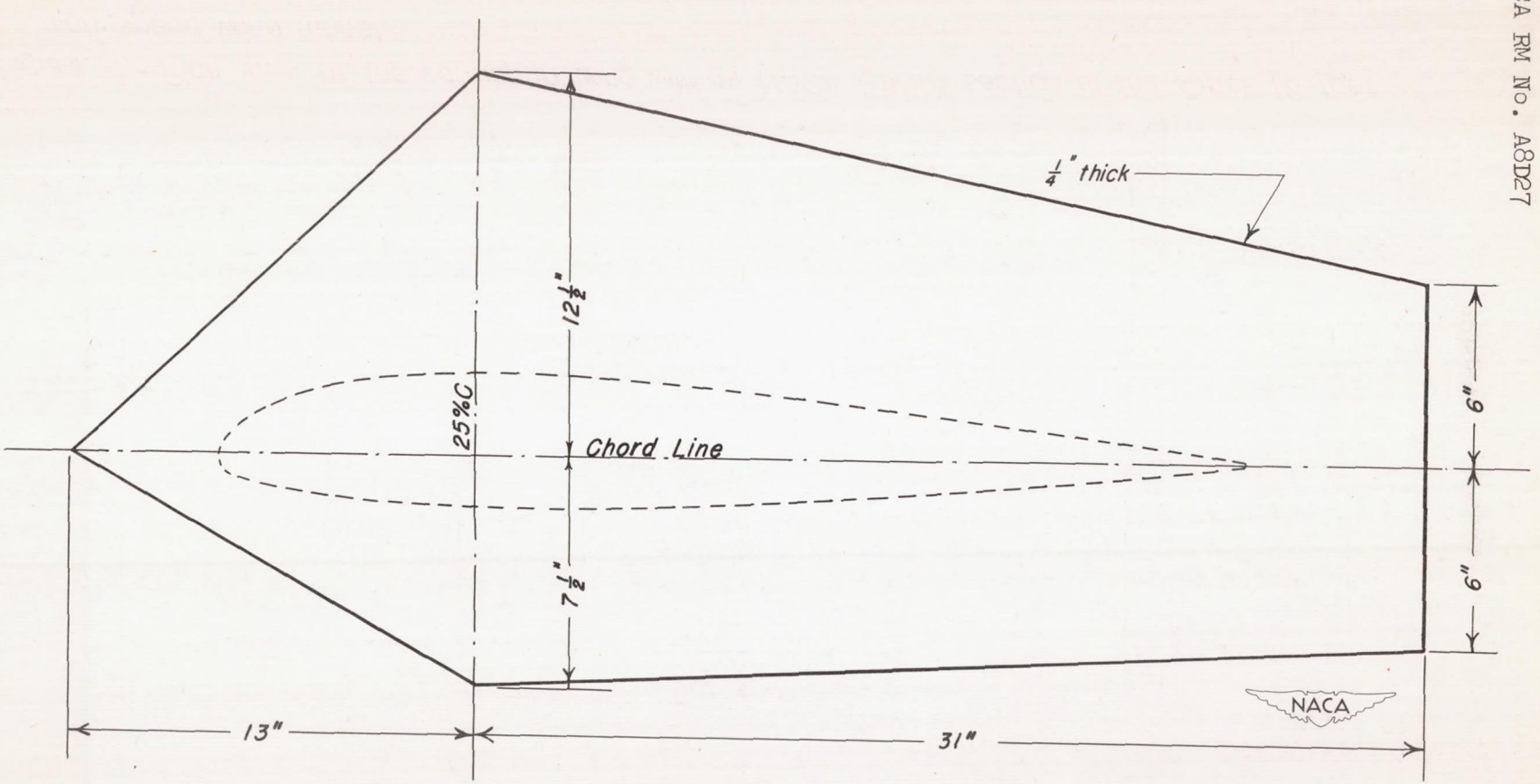

Figure 3.- Dimensions of the end plate.

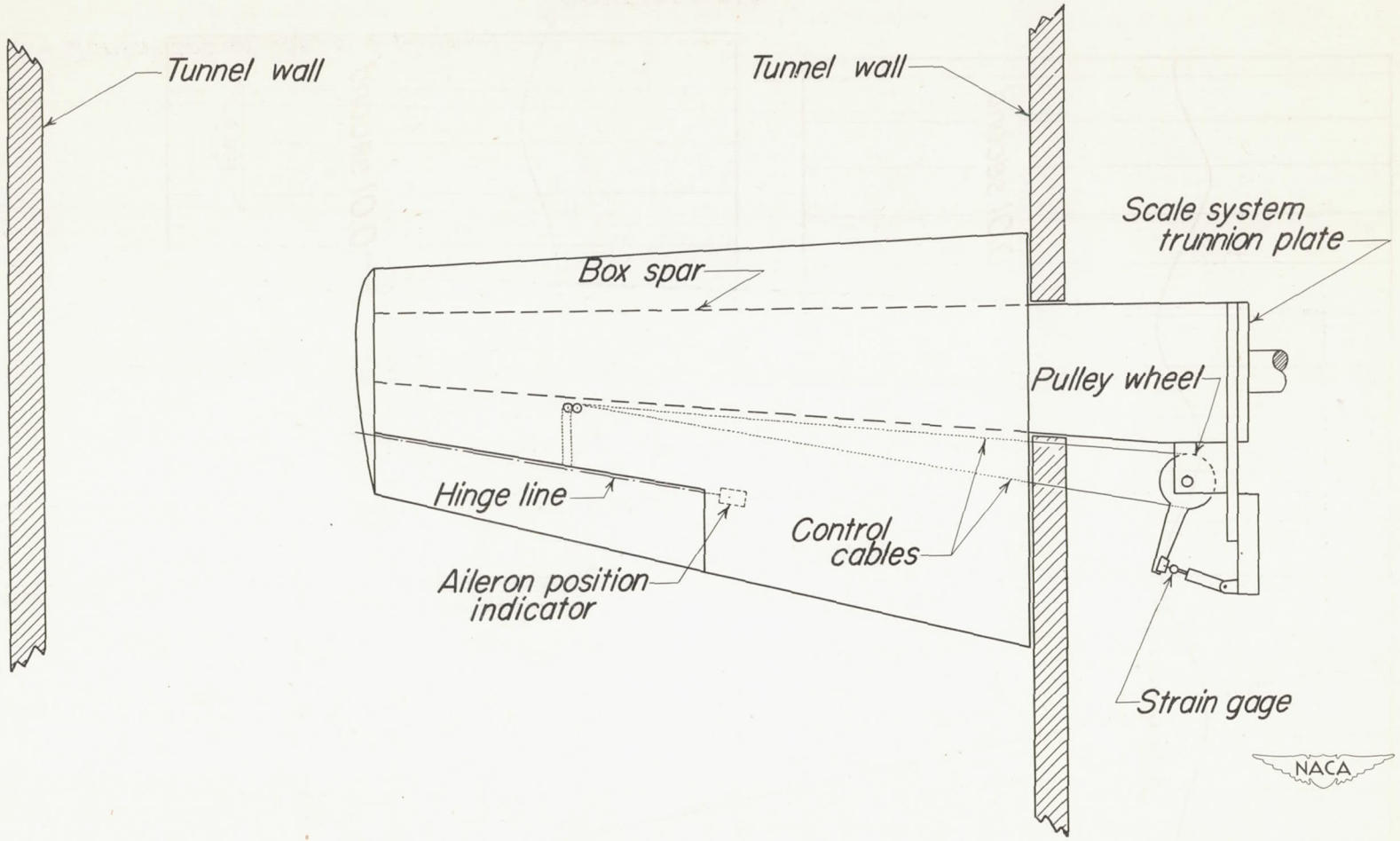

Figure 4.—Plan view of the semispan wing with an NACA 23013 section in the Ames 16-foot high-speed wind tunnel.

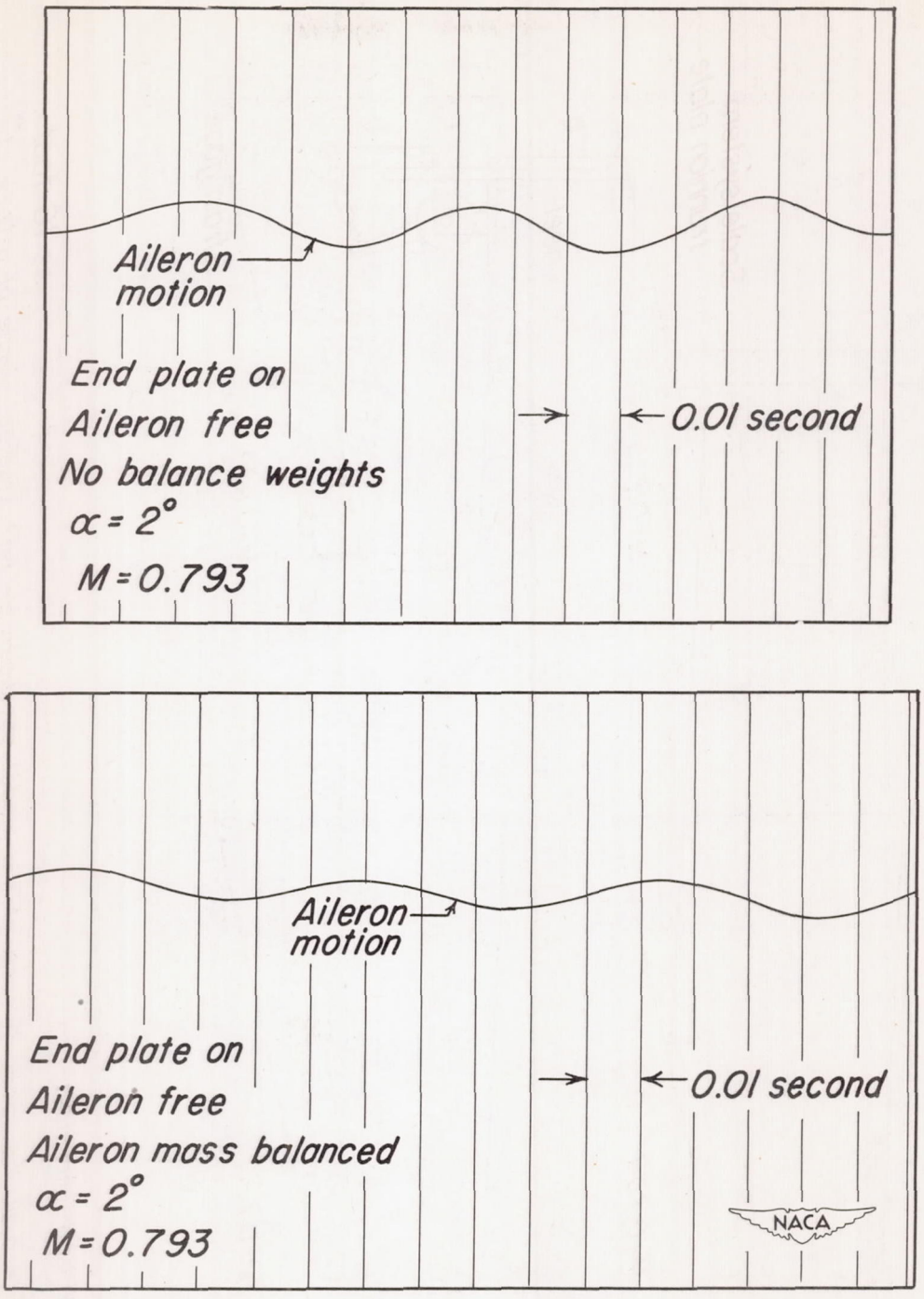

Figure 5.- Typical oscillograph records of aileron flutter.

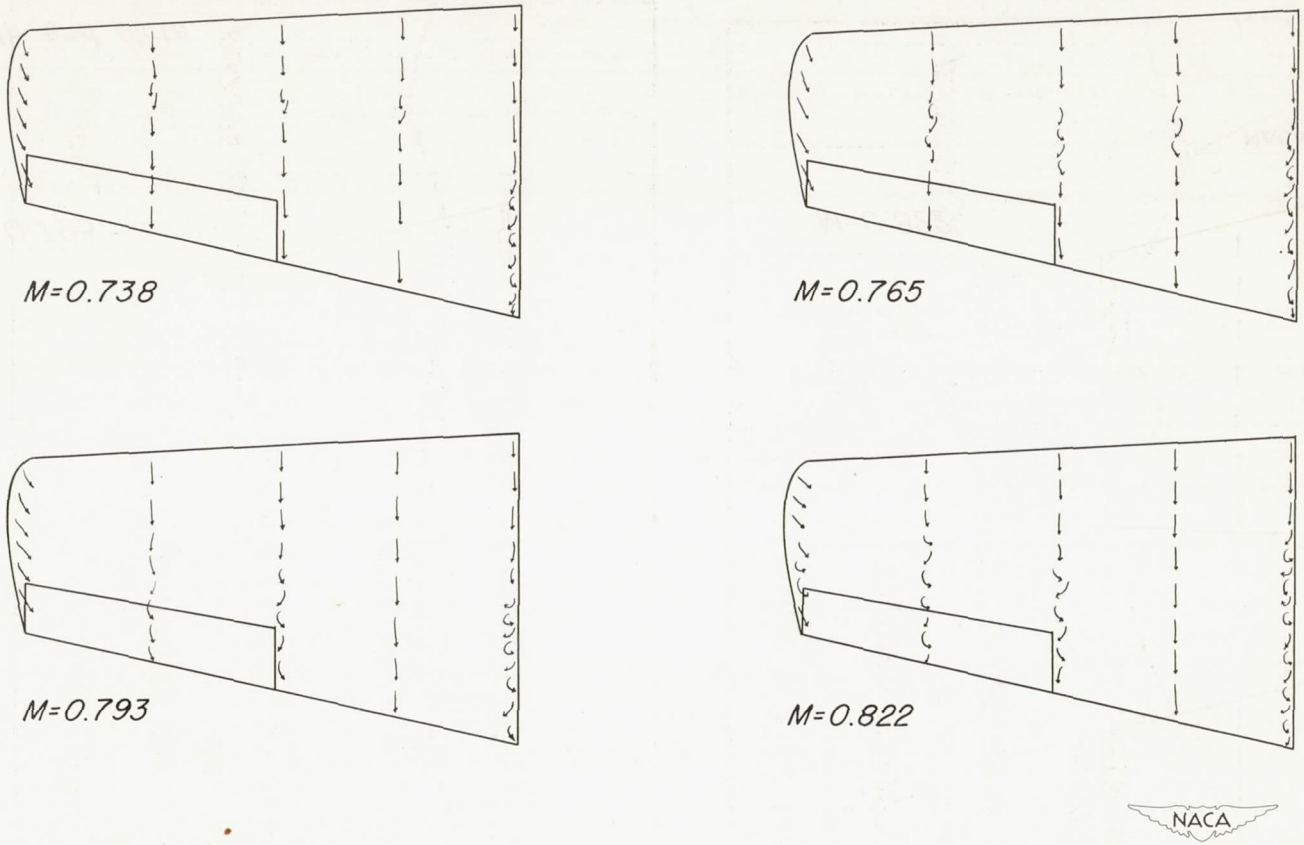

(a) Without end plate.

Figure 6.- Flow over the upper surface of the model as shown by tuft studies. Angle of attack, 1°.

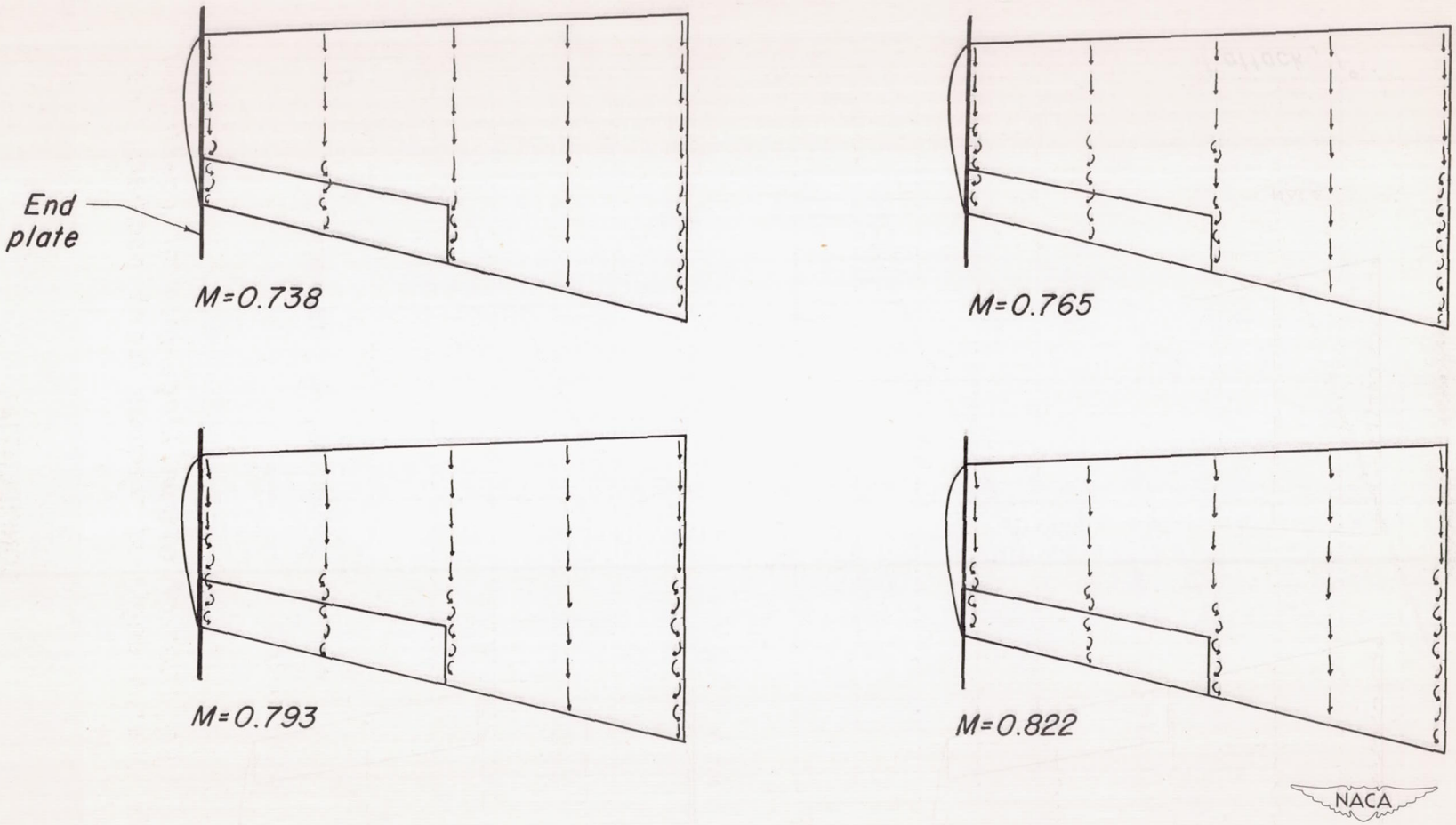

(b) With end plate.

Figure 6.– Concluded.

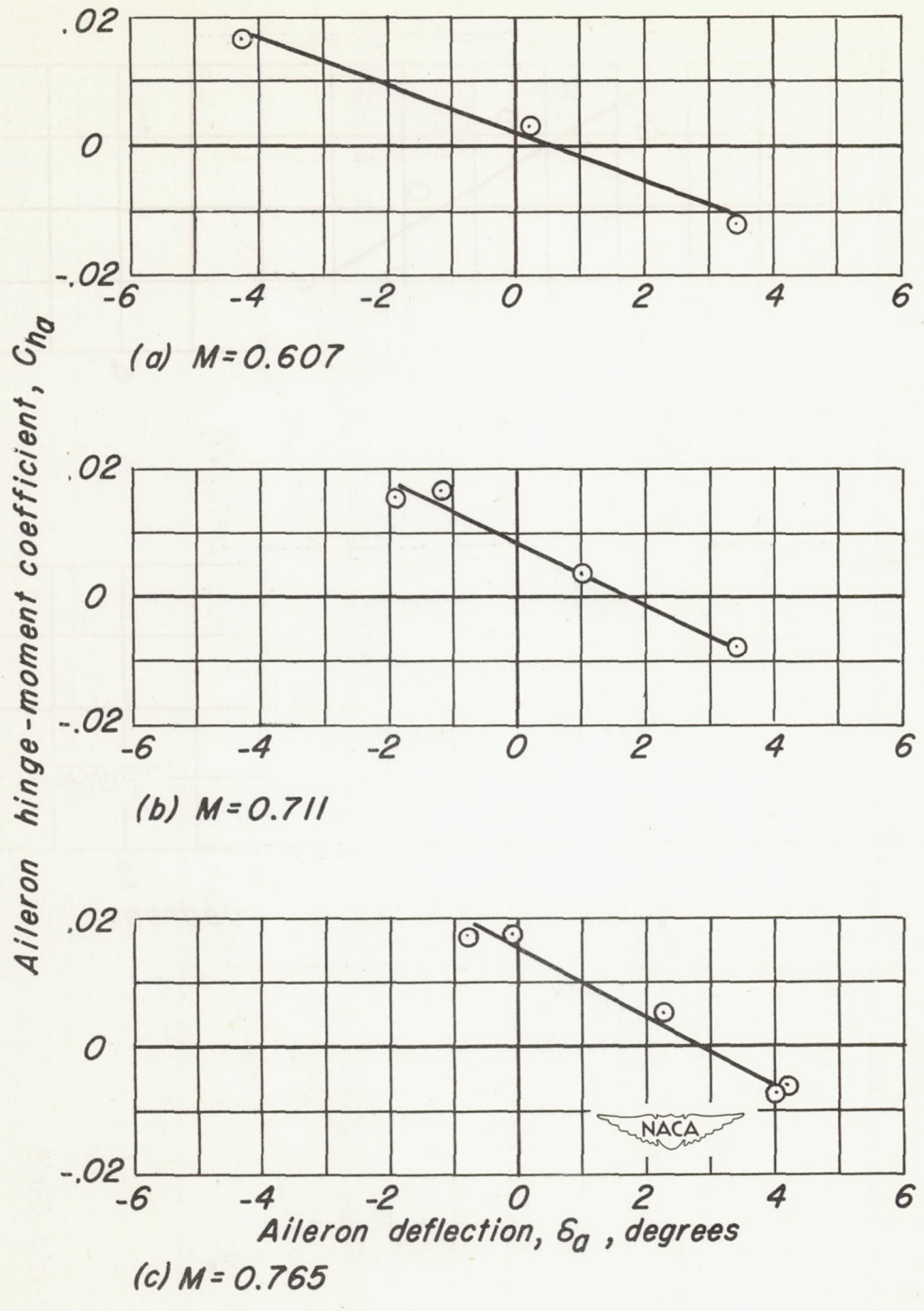

Figure.7.- Variation of aileron hinge-moment coefficient with aileron angle at various Mach numbers. End plate on.

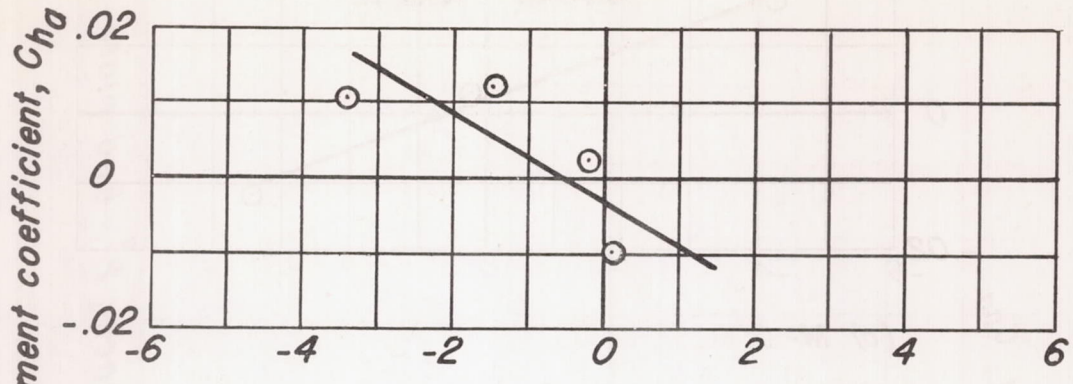

(d) M=0.793

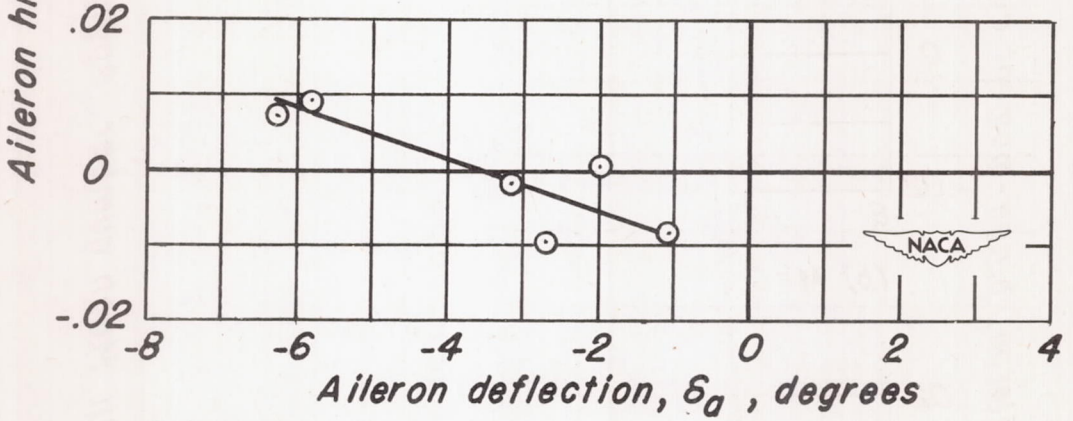

(e) M=0.822

Figure 7.- Concluded.

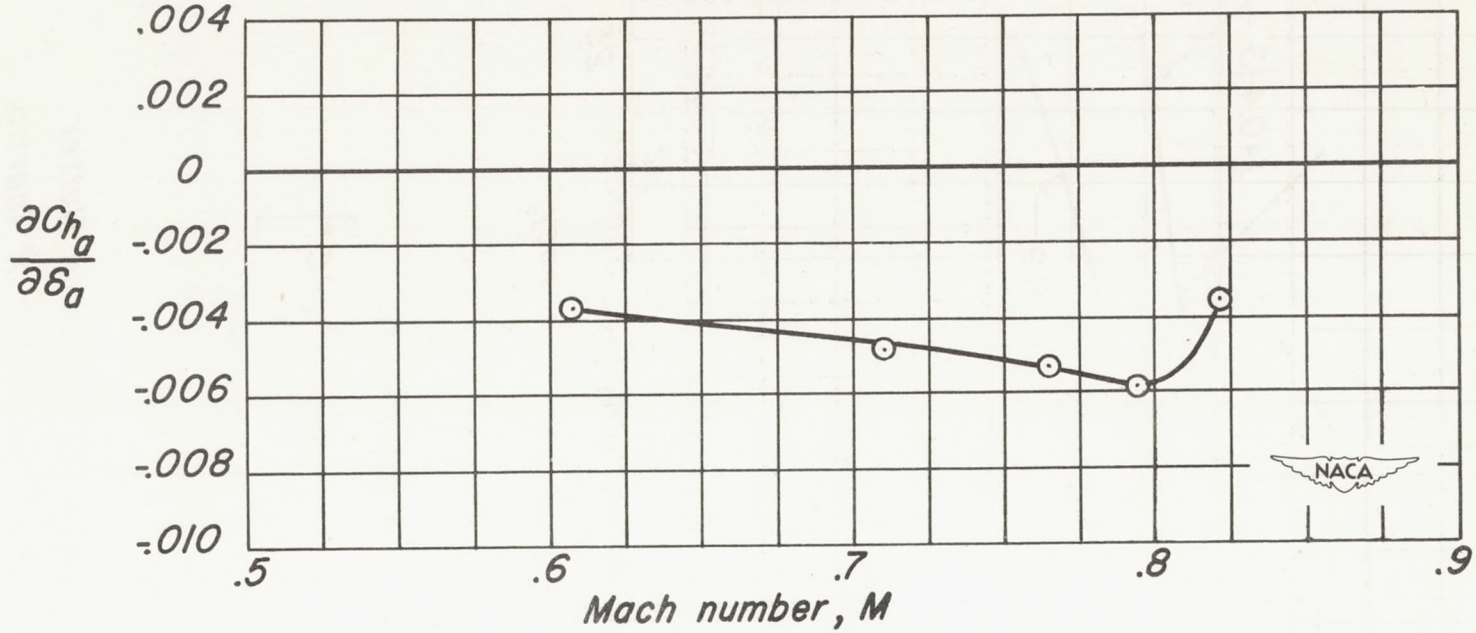

Figure 8.- Variation of $\frac{\partial C_{h_a}}{\partial \delta_a}$ with Mach number. Angle of attack, 2°. End plate on.

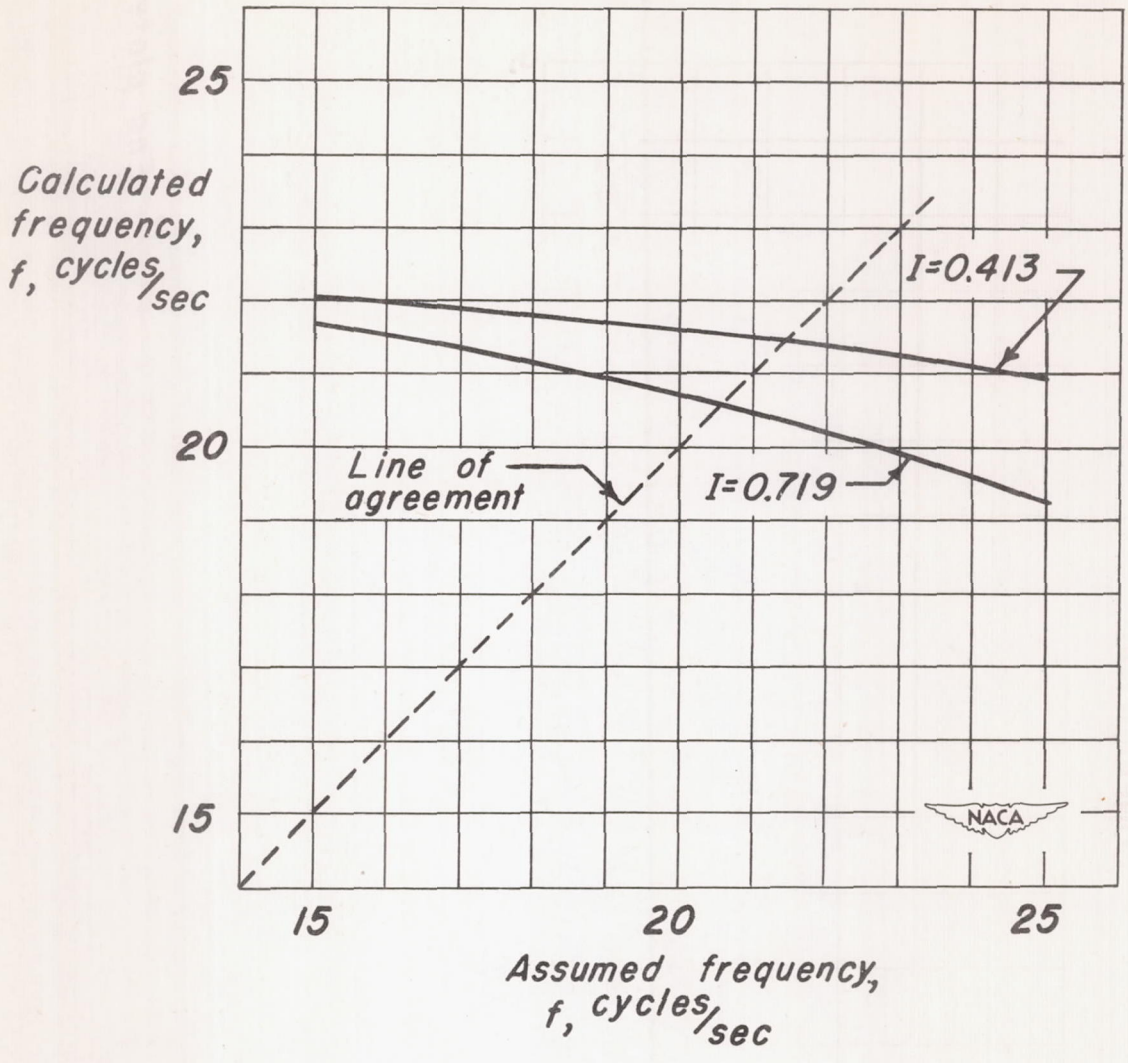

Condition for sustained flutter

$$I\omega^2 = \frac{\partial H}{\partial \delta_a} \cos\left[\left(1 - \frac{4fd}{a(1-M_{cr})}\right) 360°\right]$$

Figure 9.- Graphical solution of the aileron flutter frequency for two different moments of inertia.